Dynamic increase factor for progressive collapse analysis of semi-rigid steel frames

Yan Fei Zhu [1a], Chang Hong Chen [*1], Yao Yao [1b], Leon M. Keer [**2] and Ying Huang [3c]

[1] *School of Mechanics and Civil Engineering, Northwestern Polytechnical University, Xi'an, 710129, China*
[2] *Civil and Environmental Engineering, Northwestern University, Evanston, IL, 60286, USA*
[3] *School of Civil Engineering, Xi'an University of Architecture and Technology, Xi'an, 710055, China*

Abstract. An empirical and efficient method is presented for calculating the dynamic increase factor to amplify the applied loads on the affected bays of a steel frame structure with semi-rigid connections. The nonlinear static alternate path analysis is used to evaluate the dynamic responses. First, the polynomial models of the extended end plate and the top and seat connection are modified, and the proposed polynomial model of the flush end plate connection shows good agreement as compared with experimental results. Next, a beam model with nonlinear spring elements and plastic hinges is utilized to incorporate the combined effect of connection flexibility and material nonlinearity. A new step-by-step analysis procedure is established to obtain quickly the dynamic increase factor based on a combination of the pushdown analysis and nonlinear dynamic analysis. Finally, the modified dynamic increase factor equation, defined as a function of the maximum ratio value of energy demand to energy capacity of an affected beam, is derived by curve fitting data points generated by the different analysis cases with different column removal scenarios and five types of semi-rigid connections.

Keywords: progressive collapse; dynamic increase factor; alternate path method; nonlinear static analysis; semi-rigid steel frame

1. Introduction

Numerous studies have been made to resist progressive collapse since the gas explosion event of the Ronan Point building in 1968 (Marjanishvili and Agnew 2006, Tsai 2012, Liu 2016, Arshian and Morgenthal 2017). Development of practical and efficient approaches to protect frame structures from progressive collapse under catastrophic events (e.g., gas explosions, vehicular collisions, sabotage, fires, extreme environmental effects, human errors in design and construction) has been a significant issue in the last decade (Marjanishvili and Agnew 2006, Liu 2016, Mirtaheri and Zoghi 2016). Relevant guidelines (DOD 2009 and GSA 2013) have become available to address progressive collapse in design of frame structures.

Four different analysis methods (i.e., linear static, nonlinear static, linear dynamic, and nonlinear dynamic) are available for progressive collapse analysis of frame structures upon sudden removal of critical structural elements such as columns. The nonlinear dynamic analysis is the most accurate yet the most expensive method, because the analysis procedure is required to account for all possible types of nonlinearities; in addition, intensive computation with the time-history transient analysis is needed to simulate directly the dynamic behaviour of the damaged structure (Li *et al.* 2014, Khuyen and Iwasaki 2016). The nonlinear static analysis, incorporating an alternate path method with a dynamic increase factor (DIF), to form the impact loads, is an alternative practical approach for the analysis without using dynamic analysis (Tsai 2010, Tavakoli and Kiakojouri 2013, Chen *et al.* 2016a, b, Mashhadiali *et al.* 2016, Liu 2016).

Research has indicated that a constant DIF of 2.0 applied in the nonlinear static analysis may lead to results inconsistent with those obtained from the nonlinear dynamic analysis approach (Tsai 2010, Tavakoli and Kiakojouri 2013, Liu 2016, Mashhadiali *et al.* 2016). It should be noted that the actual nonlinear responses, as affected by both energy demand to support upper structure after removal of a column and structural capacity, is not fully considered in the DIF formulation of the DOD (2009) guidelines for steel frame structures, as defined by

$$DIF = 1.08 + \frac{0.76}{\theta_{pra}/\theta_y + 0.83} \tag{1}$$

where, θ_y and θ_{pra} are the yield rotation and the allowed plastic rotation angle, respectively, given in the acceptance criterion table of the guidelines.

It is easily understood that if the damaged structure has

∗Corresponding author, Associate Professor,
  E-mail: changhong.chen@nwpu.edu.cn
∗∗ Corresponding author, Professor,
   E-mail: l-keer@northwestern.edu
[a] Ph.D. Student, E-mail: zhuyanfei@mail.nwpu.edu.cn
[b] Professor, E-mail: yaoy@nwpu.edu.cn
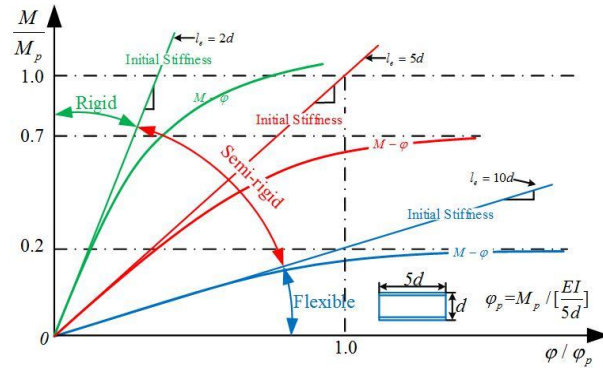[c] Associate Professor, E-mail: cch-by@163.com

Fig. 1 Non-dimensional classification of initial stiffness and ultimate strength of connections

(a) Single web angle

(b) Double web angle

(c) Header plate

(d) Top and seat angle

(e) T-Stub

(f) Top and seat angle with double web angles

(g) End plate without column stiffeners
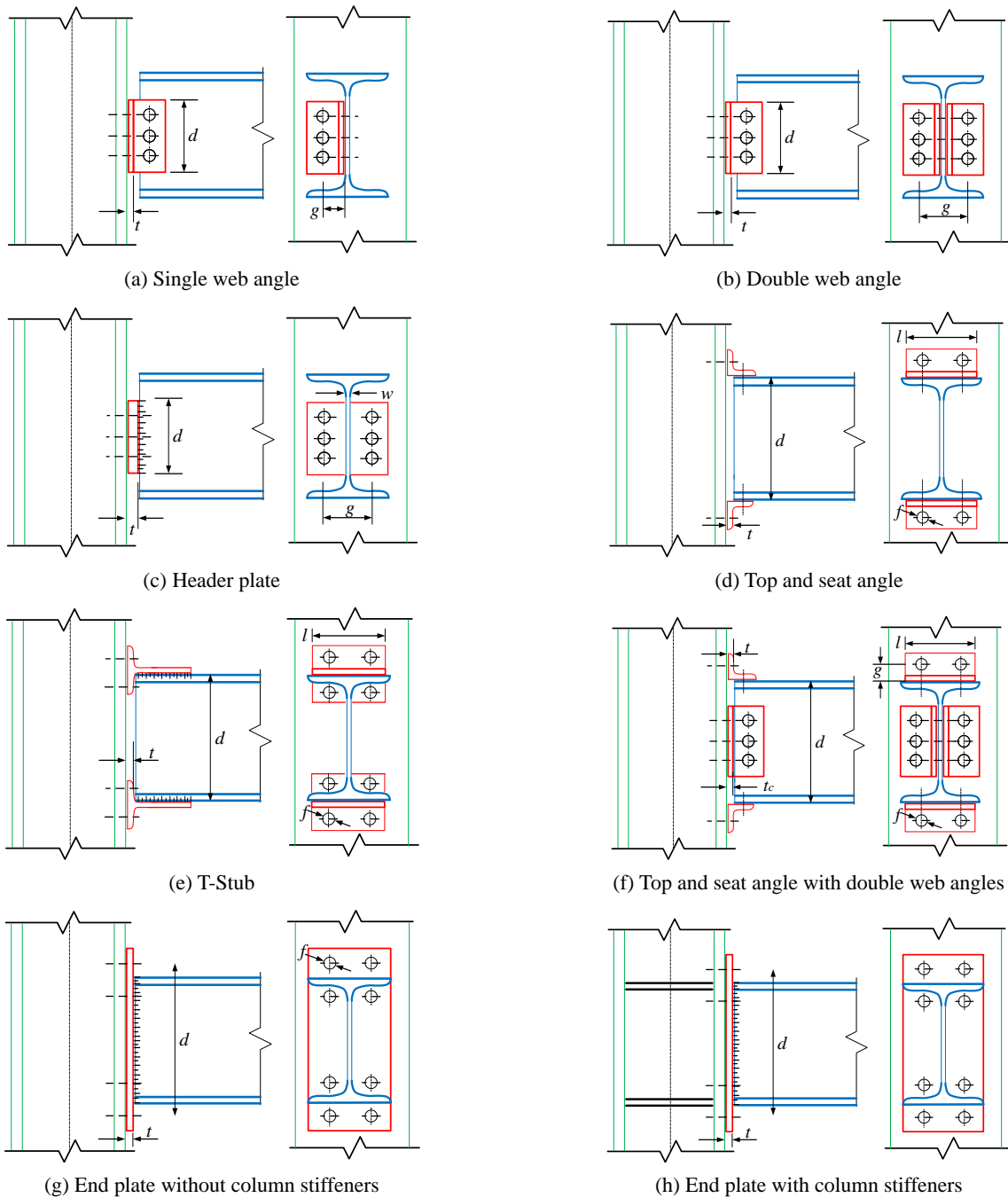
(h) End plate with column stiffeners

Fig. 2 Types of beam-to-column semi-rigid connections (Frye and Morris, 1975).

a smaller capacity and/or is subjected to greater energy demand, it would be more susceptible to progressive collapse. Furthermore, in conventional DIF analysis, beam-column connections behaviour is usually assumed for simplicity to be either perfectly rigid or ideally pinned (flexible) (Bjorhovde *et al*. 1990, Chan and Chui 2000, Degertekin and Hayalioglu 2004). Generally, it is practically impossible to achieve the widely used assumption of a perfectly rigid and frictionless pinned beam-column connection (Jones *et al*. 1983, Ihaddoudene *et al*. 2009). Connection deformation is sometimes also responsible for a substantial proportion of the overall deflection of a structure and often has a significant bearing on the internal force distribution (Frye and Morris 1975, Qin *et al*. 2016, Fu *et al*. 2017). This deformation is significant for assessing the real dynamic behaviour of a frame structure with semi-rigid connections (Frye and Morris 1975, Ihaddoudene *et al*. 2009). Therefore, it is necessary to modify the DIF for the nonlinear static analysis so that the produced static responses can more rationally match the affected dynamic responses.

A modified method for empirically calculating the DIF to assess the progressive collapse of a steel frame structure in the nonlinear static alternate path analysis is presented in the current study. The modified DIF takes into account both energy demand and structural capacity after removal of a column. The effect of connection flexibility on dynamic behaviour is also incorporated in the modified empirical DIF equation, and a step-by-step analysis procedure to obtain the modified DIF equation is developed. Specifically, a planar analytical structural model with semi-rigid connections is created to account for both connection nonlinearity by nonlinear spring elements and material nonlinearity by assigning concentrated plastic hinges in the SAP2000 program.

2. Connection behavior

2.1 Classification of connections

As previously mentioned, it is important that the connection categories can represent realistic and practical types of joints. Three basic response groups are flexible connections (pinned), rigid connections (fixed) and semi-rigid connections (Frye and Morris 1975).

Based on the evaluation of a variety of beam-to-column connections, as presented by Bjorhovde *et al*. (1990), the stiffer the connection, the shorter the equivalent reference length of the beam will be. The reference length l_e of five times the beam depth d is the most appropriate for
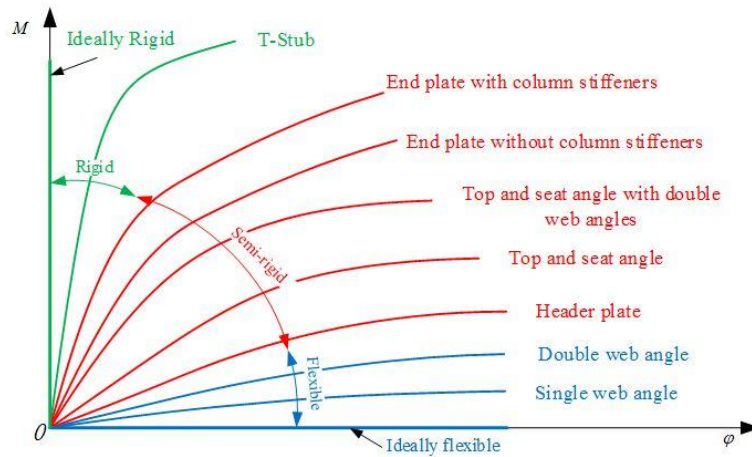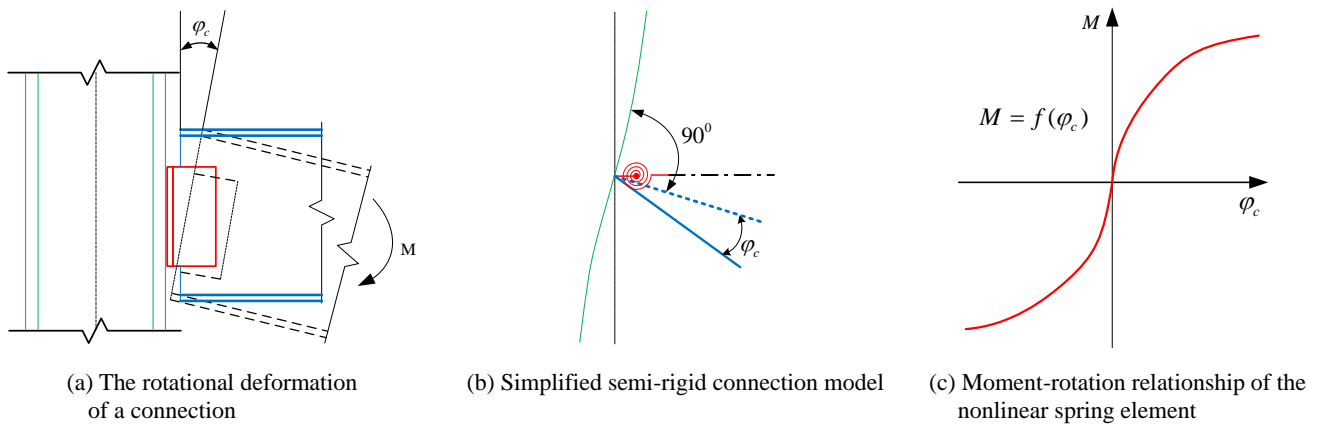

Fig. 3 Connection moment-rotation curves

(a) The rotational deformation of a connection

(b) Simplified semi-rigid connection model

(c) Moment-rotation relationship of the nonlinear spring element

Fig. 4 Design moment-rotation characteristic of a connection

semi-rigid connection, namely, δ. Also, the reference lengths of 10d and 2d, respectively, for the dividing lines between rigid and semi-rigid and between semi-rigid and flexible are proposed, namely, $l_{e,r} = 2d$ and $l_{e,f} = 10d$, as shown in Fig. 1.

It is realistic to use ultimate moment magnitudes of $0.2M_p$ and $0.7M_p$, respectively, for the flexible to semi-rigid and the semi-rigid to rigid connection strength boundaries. For rigid connections, the ultimate bending moment boundary is higher than $0.7M_p$, or perhaps even larger than the plastic moment of the attached beam M_p. The latter value reflects a design principle for occurrence of failures away from the connection regions, as shown in Fig. 1.

Types of commonly used connections with the geometry and size parameters are shown in Fig. 2 (Saberi *et al.* 2014). Many experiments have shown that practical connections behave nonlinearly due to gradual yielding of connection plates and cleats, bolts etc. (Chan and Chui 2000).

The moment-rotation curves for the eight commonly used connection types are shown in Fig. 3 presented by Frye and Morris (1975). It can be seen that flexible connection types exhibit nonlinear behaviour almost at the start of loading, while relatively rigid connections do so at a later stage.
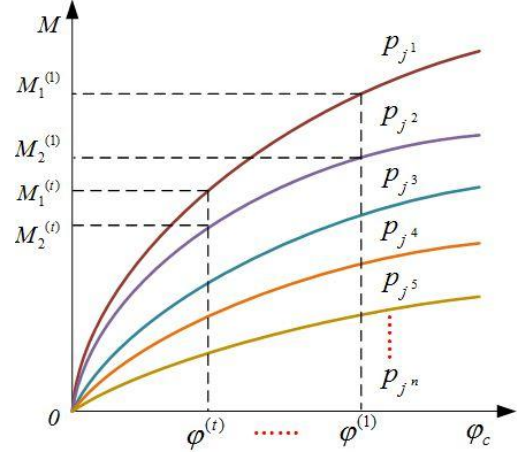

Fig. 5 Moment-rotation curves for connections with different values p_i

2.2 Properties of connections

The properties of connections are complex and uncertain. For most connections, however, the axial and shear deformations are usually small compared to flexural

Table 1 Standardized constants of the polynomial model (Frye and Morris 1975)

Connection type	Curve-fitting coefficients	Standardized constant
Single web angle	$C_1 = 4.28 \times 10^{-3}$ $C_2 = 1.45 \times 10^{-9}$ $C_3 = 1.51 \times 10^{-16}$	$K = d^{-2.4} t^{-1.81} g^{0.15}$
Double web angle	$C_1 = 3.66 \times 10^{-4}$ $C_2 = 1.15 \times 10^{-6}$ $C_3 = 4.57 \times 10^{-8}$	$K = d^{-2.4} t^{-1.81} g^{0.15}$
Header plate	$C_1 = 5.1 \times 10^{-5}$ $C_2 = 6.2 \times 10^{-10}$ $C_3 = 2.4 \times 10^{-13}$	$K = d^{-2.3} t^{-1.6} g^{1.6} \omega^{0.5}$
Top and seat angle	$C_1 = 8.46 \times 10^{-4}$ $C_2 = 1.01 \times 10^{-4}$ $C_3 = 1.24 \times 10^{-8}$	$K = t^{-0.5} d^{-1.5} f^{-1.1} l^{-0.7}$
T-stub	$C_1 = 2.1 \times 10^{-4}$ $C_2 = 6.2 \times 10^{-6}$ $C_3 = -7.6 \times 10^{-9}$	$K = d^{-1.5} t^{-0.5} f^{-1.1} l^{-0.7}$
Top and seat angle with double web angles	$C_1 = 2.23 \times 10^{-5}$ $C_2 = 1.85 \times 10^{-8}$ $C_3 = 3.19 \times 10^{-12}$	$K = d^{-1.287} t^{-1.128} t_c^{-0.415} l^{-0.649} g^{1.35}$
End plate without column stiffeners	$C_1 = 1.83 \times 10^{-3}$ $C_2 = -1.04 \times 10^{-4}$ $C_3 = 6.38 \times 10^{-6}$	$K = d^{-2.4} t^{-0.4} f^{1.1}$
End plate with column stiffeners	$C_1 = 1.79 \times 10^{-3}$ $C_2 = 1.76 \times 10^{-4}$ $C_3 = 2.04 \times 10^{-4}$	$K = d^{-2.4} t^{-0.6}$

deformations. For simplicity, only the rotational behaviour of connections due to flexural action is considered, and the catenary action is not taken into account in the current study. The design moment-rotation characteristic of a connection is shown in Fig. 4.

The standardization procedure representing the moment-rotation curves for all connections of a given type proposed by Frye and Morris (1975) is expressed as a single function

$$\varphi = \sum_{i=1}^{\infty} C_i (KM)^i \tag{2}$$

where φ is a rotational deformation of connection in radians, C_i is curve-fitting constant, K is a dimensionless standardization constant, depending on the size parameters for the particular connection, and M is the moment applied to the connection.

The slope of the curve, namely, the tangent connection stiffness, S_c, is given by

$$S_c = \frac{dM}{d\varphi} \tag{3}$$

and the initial stiffness S_c^0 is given by

$$S_c^0 = \frac{dM}{d\varphi}\bigg|_{M=0} = \frac{1}{C_1 K} \tag{4}$$

The factor K is given by

$$K = \prod_{j=1}^{m} p_j^{a_j} \tag{5}$$

where p_j is numerical value of jth size parameter, a_j is a dimensionless exponent indicating the effect of jth size parameter on the moment-rotation relationship, and m is total number of size parameters. The value of the exponents a_j in Eq. (5) can be illustrated by a series of experimental moment-rotation curves for connections, and as given by

$$a_j = \frac{\log(M_1 / M_2)}{\log(p_{j^2} / p_{j^1})} \tag{6}$$

In addition, a_j values are calculated by several different rotations for each combination of experimental curves, as shown in Fig. 5, and as expressed by

$$a_j = \bar{a}_j = \frac{1}{\eta} \cdot \frac{1}{t} \cdot \sum_t \sum_{a \neq \beta}^{n} \frac{\log(M_1^{(t)} / M_2^{(t)})}{\log(p_{j\alpha} / p_{j\beta})} \tag{7}$$

where, t is the selected rotation number in each of experimental curves; n is the number of experimental curves; η is a combinatorial number of the different experimental curves, namely, $\eta = n! / [2(n-2)!]$; $p_{j\alpha}$ and $p_{j\beta}$ represent different p_j corresponding to the different experimental curves, respectively.

Based on the test data, standardized moment-rotation functions for each of the eight connection types shown in Fig. 2 are listed in Table 1 determined by Frye and Morris (1975).

3. A modified DIF calculation method

3.1 The modified polynomial model of partial connections

Based on the experimental results (Yang and Tan 2012, 2013) and the results shown in Table 1, the influence of the middle bolts in the extended end plate (EEP) connections on the moment-rotation capacity is not considered in the researches by Frye and Morris (1975). The polynomial model of the flush end plate (FEP) connections has also not been determined. Therefore, the polynomial model of the extended end plate connections and of the flush end plate connections are respectively modified and proposed. A modified model of the top and seat (TS) connections is also provided in the current paper.

Details and standardization parameters for extended end plate connections with column stiffeners are shown in Fig. 6. Some key techniques of modeling the finite element model of the extended end plate connections are presented by Yang and Tan (2012) (similarly hereinafter). Based on FEM numerical simulation analysis results by the ABAQUS software, as shown in Figs. 7-9, corresponding to the different values f, t and d_2, respectively, the polynomial model of the extended end plate connections is modified and given by Eqs. (8)-(9)
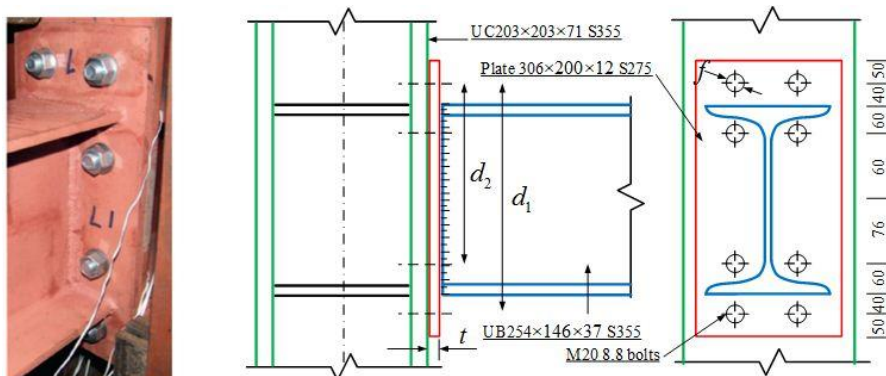

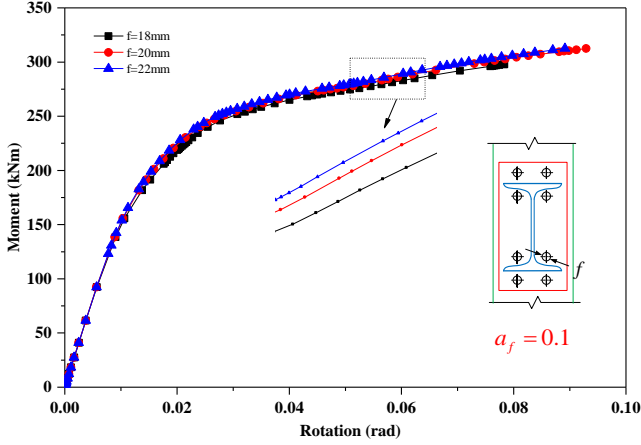Fig. 6 Details and standardization parameters for extended end plate connections with column stiffeners

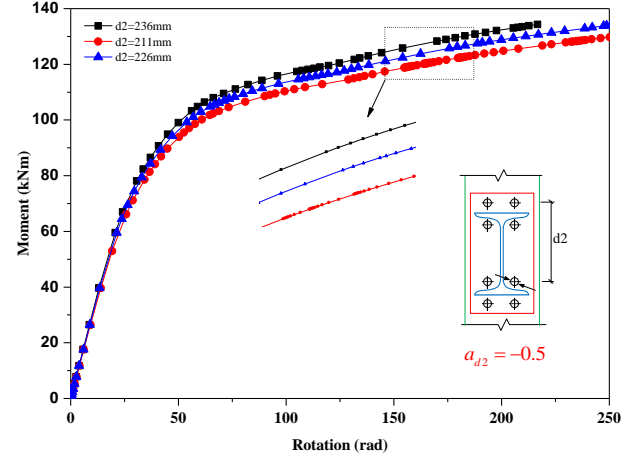Fig. 7 Moment-rotation curves for extended end plate connections with different values f

Fig. 9 Moment-rotation curves for extended end plate connections with different values d_2
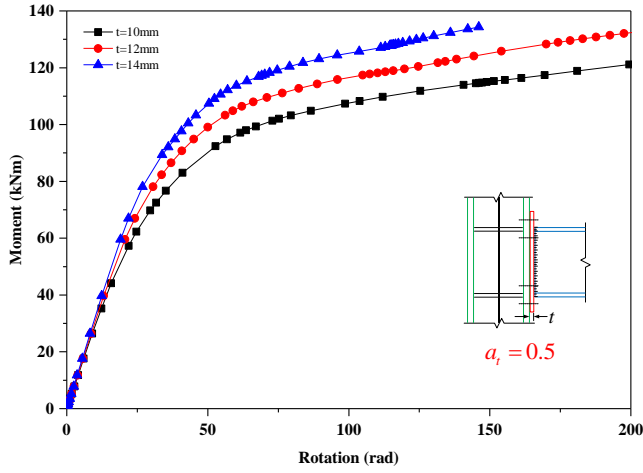

Fig. 8 Moment-rotation curves for extended end plate connections with different values t
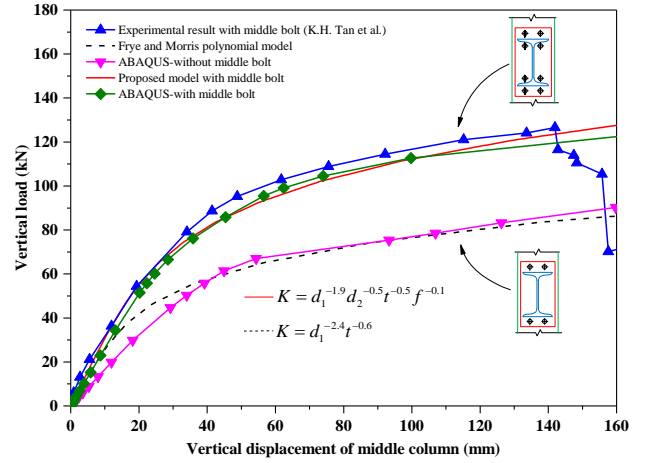

Fig. 10 Comparison of the FEM simulations to the test data of extended end plate connections

$$K = d_1^{-1.9} d_2^{-0.5} t^{-0.5} f^{-0.1} \tag{8}$$

$$\begin{aligned} C_1 &= 1.06 \times 10^{-3} \\ C_2 &= 3.61 \times 10^{-5} \\ C_3 &= 1.45 \times 10^{-5} \end{aligned} \tag{9}$$

The polynomial model of the extended end plate connections modified in the current study shows good agreement compared with experimental results, as shown in Fig. 10.

Details and standardization parameters for flush end plate connections with column stiffeners are shown in Fig. 11. Similarly, based on FEM numerical simulation analysis results by the ABAQUS software, the polynomial model of the flush end plate connections is proposed and given by
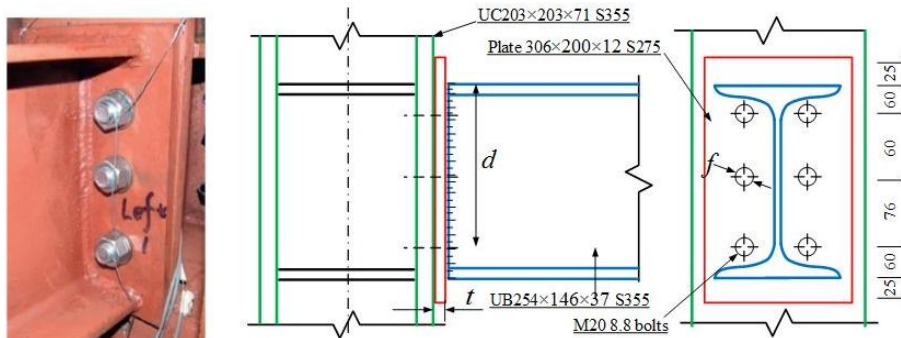
$$K = d^{-1.1} t^{-0.4} f^{-0.2} \tag{10}$$

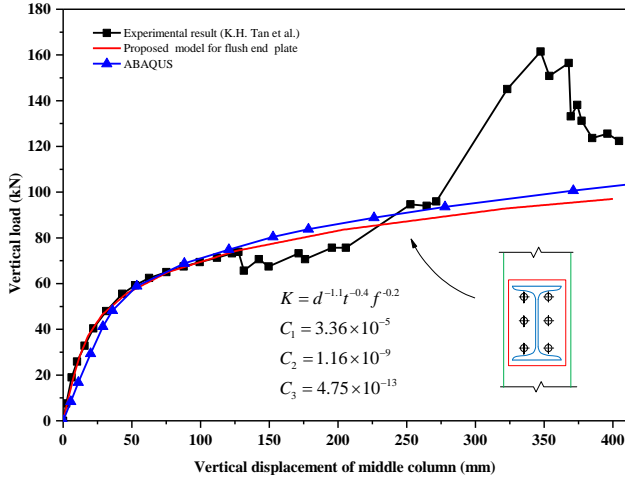Fig. 11 Details and standardization parameters for flush end plate connections with column stiffeners

Fig. 12 Comparison of the FEM simulations to the test data of flush end plate connections

$$C_1 = 3.36 \times 10^{-5}$$
$$C_2 = 1.16 \times 10^{-9} \qquad (11)$$
$$C_3 = 4.75 \times 10^{-13}$$

The modified polynomial model of the flush end plate connections in the current study shows good agreement compared with experimental results, as shown in Fig. 12.

Details and standardization parameters for top and seat connections with column stiffeners are shown in Fig. 13. The simulation analysis results from the polynomial model proposed by Frye and Morris (1975) appear different from the experimental results obtained by Yang (Yang and Tan 2012, 2013), as shown in Fig. 14. Based on the experimental results by Yang (Yang and Tan 2012, 2013), a polynomial model of the top and seat connections is modified and given by

$$K = t^{-1.99} d^{-1.5} f^{-1.1} l^{-0.7} \qquad (12)$$

$$C_1 = 8.21 \times 10^{-4}$$
$$C_2 = 8.90 \times 10^{-7} \qquad (13)$$
$$C_3 = 1.37 \times 10^{-10}$$

The modified polynomial model of the top and seat connections in the current study shows good agreement compared with experimental results, as shown in Fig. 14.

3.2 A beam model with nonlinear spring elements and plastic hinges

In order to incorporate the combined effect of joint flexibility and material yielding on the structural dynamic
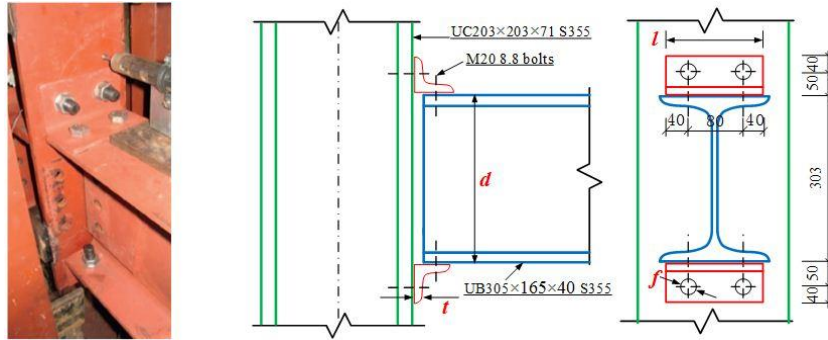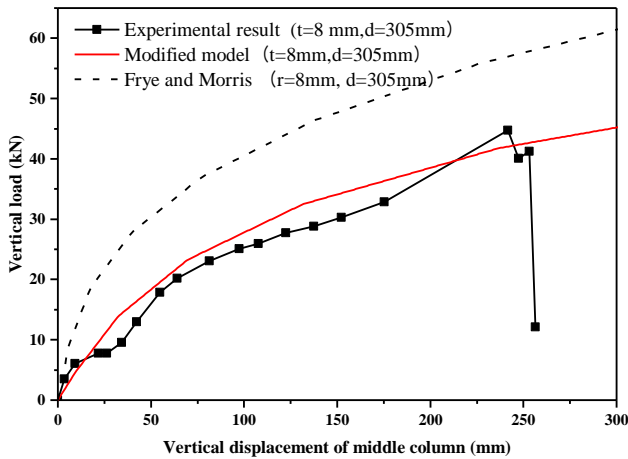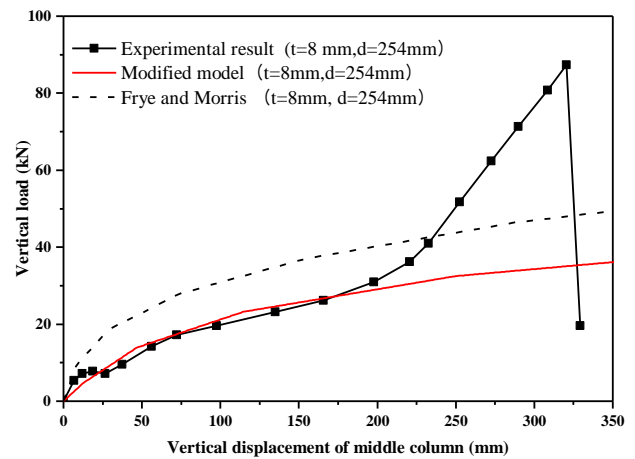

Fig. 13 Details and standardization parameters for top and seat connections
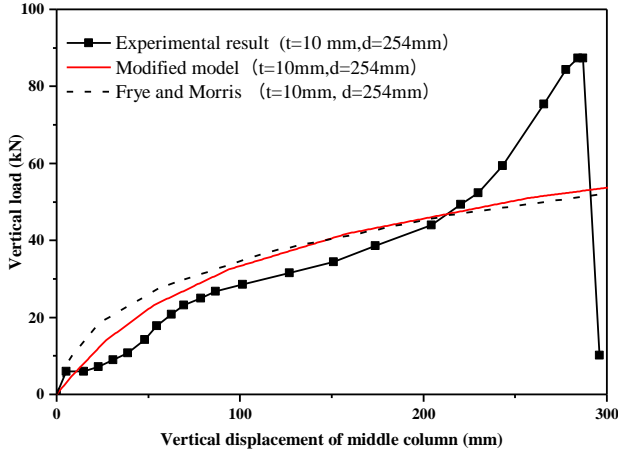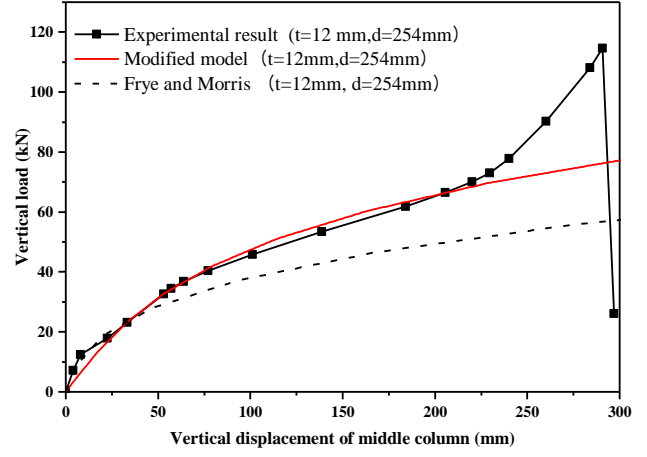

(a) Specimen 1

(b) Specimen 2

Fig. 14 Comparisons of the modified model to the test data of top and seat connections

(c) Specimen 3

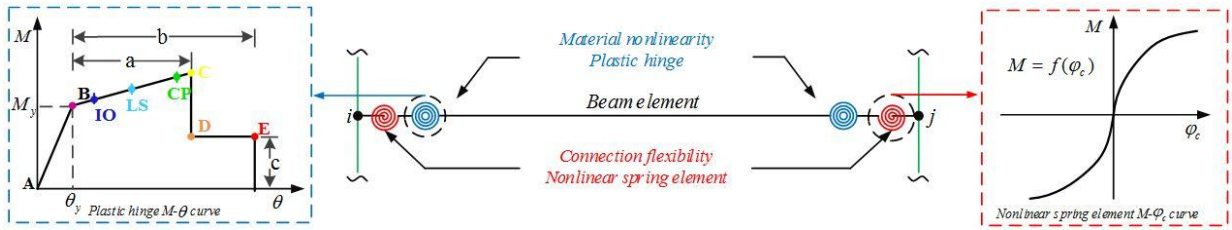(d) Specimen 4

Fig. 14 Continued

Fig. 15 Beam-column element attached with section and connection springs

response, a compound beam-column element established by SAP2000 software with plastic hinge for material nonlinearity and with nonlinear spring element for semi-rigid connection is utilized in the current study, as shown in Fig. 15. The moment-rotation relation for beam plastic moment hinges is obtained based on the Federal Emergency Management Agency (FEMA) 356 (2000), where the Immediate Occupancy, Life Safety and Collapse Prevention structural performance levels are determined. The plastic deformations (a and b) and the residual strength (c), as shown in Fig. 15, are assessed based on the FEMA 356 (2000). The flexural strength is calculated by

$$M_y = Zf_{ye} \qquad (14)$$

And the rotation at yield is

$$\theta_y = \frac{Zf_{ye}L_b}{6EI_b} \qquad (15)$$

where f_{ye} is the expected material yield strength; L_b is beam length; Z is plastic section modulus; I_b is a moment of inertia, and E is the modulus of elasticity.

Total rotation (θ), as shown in Fig. 16, of the compound element is given by (Chan and Chui 2000)

$$\theta = \theta_c + \theta_p \qquad (16)$$

where, θ_c and θ_p stand for connection rotation and plastic hinge rotation, respectively. Elastic rotation being very
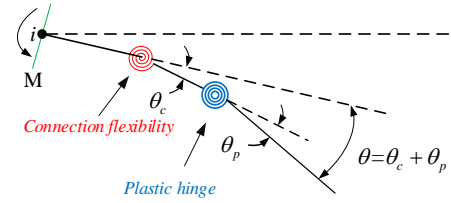

Fig. 16 Deformation exhibition of a semi-rigid connection and a plastic hinge

small is often neglected.

The three parameter power model for a semi-rigid connection (Chan and Chui 2000, Saberi *et al*. 2014), as shown in Fig. 17(a), is given by

$$\theta_c = \frac{M}{R_{ki}(1 - (M / M_u)^n)^{1/n}} \text{ or, } M = \frac{R_{ki}\theta_c}{(1 + (\theta_c / \theta_0)^n)^{1/n}} \quad (17)$$

where, R_{ki} is the previously mentioned initial connection stiffness, S_c^0 in Eq. (3), M_u is the ultimate capacity of the connection moment, n is the shape parameter and θ_0 is the reference plastic rotation given by

$$\theta_0 = \frac{M_u}{R_{ki}} \qquad (18)$$

A four parameter power model for a semi-rigid connection (Chan and Chui 2000, Jones and Kirby 1983) as shown in Fig. 17(b), is given by
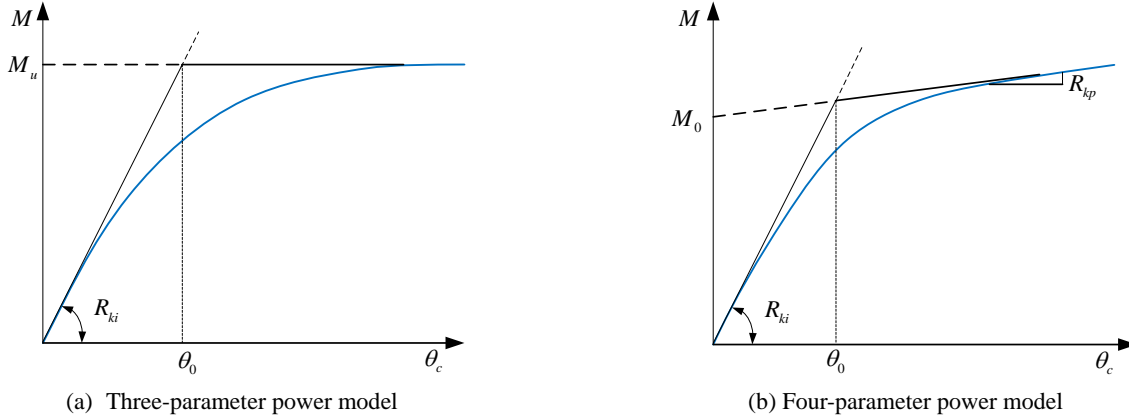
(a) Three-parameter power model

(b) Four-parameter power model

Fig. 17 The power model for semi-rigid connections

$$M = \frac{(R_{ki} - R_{kp})\theta_c}{(1 + (\theta_c / \theta_0)^n)^{1/n}} + R_{kp}\theta_c \tag{19}$$

where, R_{kp} is the strain hardening/softening stiffness and θ_0 is the reference plastic rotation given by

$$\theta_0 = \frac{M_0}{R_{ki} - R_{kp}} \tag{20}$$

where, M_0 is reference relative moment.

Based on the three and four parameter power model, the capacity of a connection can be characterized by the reference plastic rotation θ_0 (Jones *et al*. 1983, Chan and Chui 2000, Saberi *et al*. 2014). Therefore, the reference plastic rotation θ_0 is applied for the DIF assessment process in the current paper.

3.3 The DIF calculation procedure

The modified DIF is defined as a function of max (ED/EC) in the current study, where the max operator is applied to all affected beams directly adjacent to and above the removed column, and ED and EC are structural energy demand and energy capacity, defined by Eqs. (21) and (22), respectively

$$ED = M_l \times \theta = M_l \times (\theta_c + \theta_p) \tag{21}$$

$$EC = M_y \times (\theta_0 + \theta_y) \tag{22}$$

where, M_l, θ_c and θ_p are the factored moment, connection rotation and plastic hinge rotation, respectively, of an affected beam under the original unamplified static loads, θ_0 is the reference plastic rotation of a semi-rigid connection, mentioned previously, and M_y and θ_y are the expected plastic moment capacity and the yield rotation of an affected beam, expressed as Eqs. (14) and (15), respectively.

For a given column removal scenario, the DIF is obtained when the structural responses from the pushdown analysis best match those from the nonlinear dynamic analysis. The calculation process of the DIF for the damaged frame under a given column removal scenario

takes the following steps:

Step 1: Perform a nonlinear dynamic analysis to obtain the maximum vertical dynamic response displacement $\Delta_{max,ND}$ at the column removal location. To carry out the dynamic analysis, different approaches are categorized into two main groups; either direct element deletion or reaction approaches (Tavakoli and Kiakojouri 2013). A subroutine is required in the direct element deletion approaches. In the reaction approaches, a nonlinear analysis of the intact structure with the primary load *g* is carried out to record the end forces F of the to-be-removed column. The analysis then statically applies the primary load *g* and end forces F (in opposite directions) to the damaged structure model with a column removed in order that the deformation of the model is the same as the intact structure just before the damage. Once static equilibrium is reached, the end force F is instantly forced to zero to start the dynamic response time history analysis and to simulate the phenomenon of abrupt removal of a column. The maximum dynamic responses are then measured and calculated. In the current study, dynamic analysis is automatically carried out by the reaction approach using the SAP2000 program application programming interface incorporated with the Visual Basic for Applications in Excel software.

Step 2: Perform a pushdown analysis by applying an increasing vertical load *q* on the affected bays (or damaged bays) immediately adjacent to and above the removed column, and by applying a nominal design load *p* to the other bays, as shown in Fig. 18, from which the displacement at the column removal location versus applied load curves are obtained.

Step 3: Based on the responses from the nonlinear dynamic analysis, determine the time T_p when the vertical displacement obtained by pushdown analysis $\Delta_{max,P}$ reaches the Δ_{maxND}. It is understandable that the DIF is equal to T_p, i.e., $DIF = T_p$, and the DIF is calculated rapidly by the proposed method. The process differs from the traditional methods utilized by Liu (2013) and Khuyen and Iwasaki (2016).

Step 4: Determine M_l, θ_c and θ_p when the applied load in the affected bays reaches normal design load *g*, i.e., the time in pushdown analysis reaches 1.0; next find the max (ED/EC).

The above major steps for DIF calculation are illustrated

(a) Increasing load in the damaged bays (b) Nominal design load in other bays

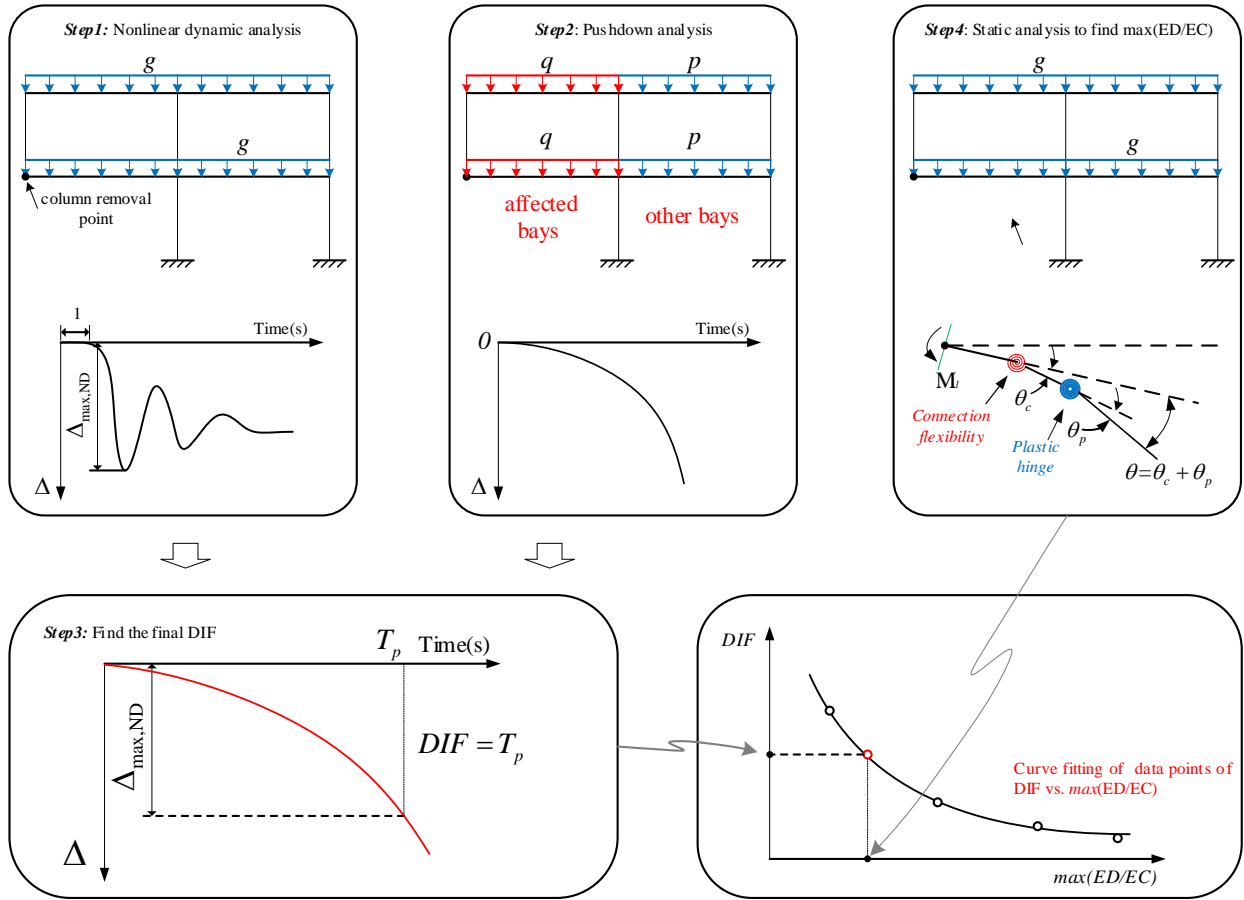Fig. 18 Load applied curve in different bays

Fig. 19 Illustration of the steps to obtain the data point of DIF vs. max (ED/EC)

in Fig. 19. After the above four steps, a data point of DIF vs. max(ED/EC) is obtained. This process is then repeated for all other column removal scenarios of the current building frame, as described in Section 4.1. Finally, curve fitting of these data points is conducted to find empirical formulas for calculating the DIF.

4. Illustrative application to steel frame structures

4.1 The analysis model

The representative building in our analysis, is a two-dimensional nine-story steel frame structure, as shown in Fig. 20, earlier studied by Liu (2013). Min Liu's frame

was rigid jointed, but in the present study, the beam column connections are semi-rigid. To observe the effect of semi-rigid connections on the DIF and progressive collapse behaviour, five different connections are adopted in the current study, as shown in Fig. 21. Grade A992Fy50 steel with a modulus of elasticity of 200 Gpa, a yield stress (F_y) of 345 Mpa (50 ksi), and effective yield stress (F_{ye}) of 379.2 Mpa (55 ksi) is used in the example. A live load is assumed to be 3.92 N/mm distributed uniformly across the entire beam span including the roof. To estimate the dead load, we assumed a uniform concrete slab thickness of 90 mm (3.5 in), with normal weight concrete density of 23.6 kN/m^3 (150 pcf). The equivalent linear load is 4.28 N/mm. Additionally, the dead load includes perimeter wall weight of 19.7 N/mm (1,350 plf) at every floor, except at roof
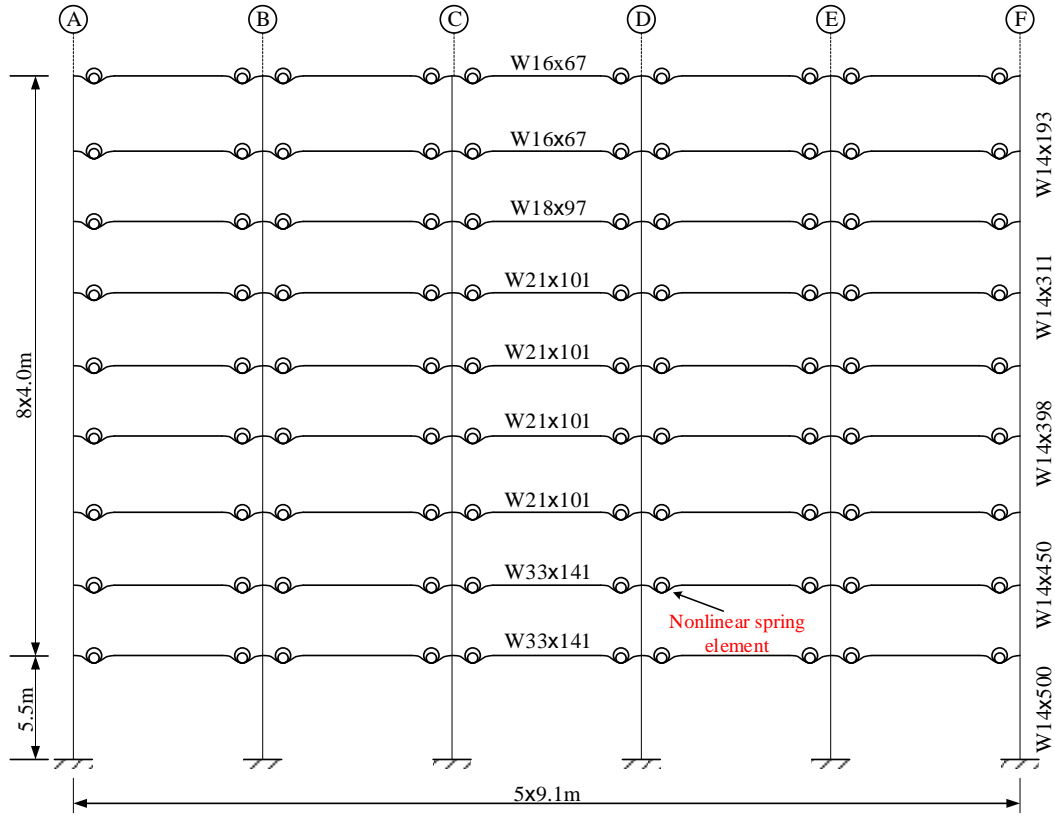
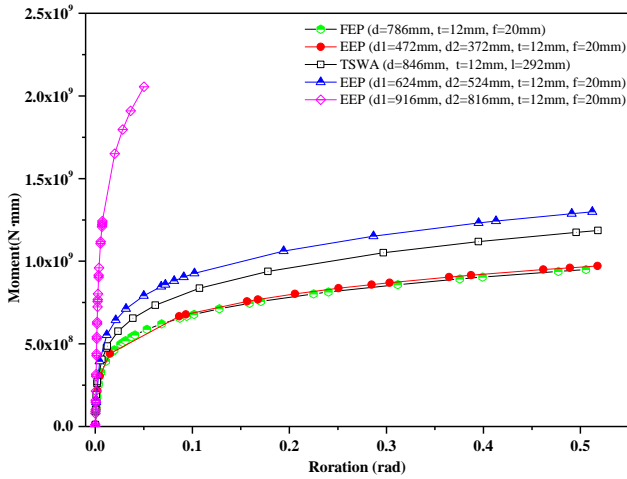Fig. 20 Two-dimensional structural model of example building

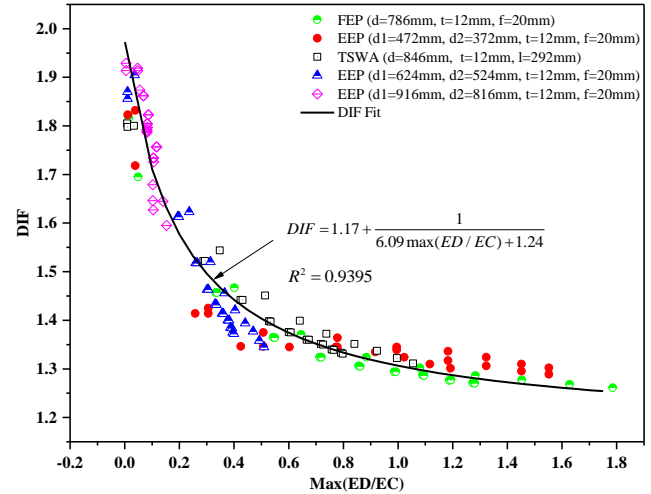Fig. 21 Moment-rotation curves of five different types of connections

Fig. 22 Dynamic increase factor as a function of max (ED/EC)

level.

Member sizes for the steel frame are shown in Fig. 20. A single section size is used for all beams at a given floor. Column members in the ground floor are W14×500; and for other stories, columns between every two adjacent floors have the same section size along each of the exterior or interior column lines.

4.2 Column fracture scenarios

All columns are subject to removal in this study to investigate completely the dynamic response of a steel frame. Due to symmetry in the frame layout, only half of the columns in each story are to be removed, one at a time. Therefore, a total of 3 × 9 = 27 different column removal scenarios are considered for each of the five steel frames with different types of connections (Liu 2016). Each of the column removal scenarios is accomplished efficiently by the SAP2000 program application programming interface incorporated with the Visual Basic for Applications in Excel software (Chen *et al*. 2016c).

4.3 Results and discussion

According to the DIF calculation procedure mentioned before, all column removal scenarios are investigated completely to analyze the load redistribution behaviour of a steel frame and to obtain the DIF formula. Fig. 22 displays the data points of the final DIF vs. max (ED/EC) of all illustrative cases. The modified empirical equation is given by

$$DIF = 1.17 + \frac{1}{6.09 \max(ED/EC) + 1.24} \qquad (23)$$

As observed in Fig. 22, the dynamic response or DIF is strongly related to the type of beam-column connection, and it is noticed that a column removal scenario with weak beam-column connections has a smaller DIF than those with strong beam-column connections. Therefore, connection flexibility should be given full consideration in the analysis and design of steel structures to resistant progressive collapse.

For a given beam-column connection, the smaller max(ED/EC) turns out to be associated with removal of a column in an upper story level. This observation could be attributed to the situation that removal of a column from an upper story causes a low level of overall geometrical nonlinearity compared with removal of a column from a lower story, thereby leading to a smaller DIF for the lower-story column removal scenario (Liu 2016).

It is worth reminding that the maximum value (DIF_{max} = 1.976) obtained by Eq. (23) of the modified DIF is close to, but less than, the constant value (DIF = 2.0) used in the traditional analysis and design. Also, the maximum and minimum values are close to the value obtained by Eq. (1) recommended in DOD (2009) guideline.

5. Conclusions

The current work focuses on evaluating the dynamic increase factor (DIF) for progressive collapse by considering the nonlinear static analysis of steel frames with semi-rigid connections. The following observations are made:

(1) The modified polynomial model of the extended end plate and top and seat connection and the proposed polynomial model of the flush end plate connection show good agreement compared with experimental results.
(2) The utilized beam-column element established by the SAP2000 program attached with plastic hinge for material nonlinearity and a nonlinear spring element for semi-rigid connection can be applied to incorporate the combined effect of joint flexibility and material yielding on the structural dynamic response.
(3) Data points of DIF vs. max (ED/EC) of all illustrative cases shows that the DIF for nonlinear static alternate path analysis is directly related to both energy demand and structural capacity.

(4) The modified empirical DIF equation is incorporated in the effect of connection flexibility on the dynamic behaviour of the damaged structure after abrupt removal of a column.

References

Arshian, A.H. and Morgenthal, G. (2017), "Three-dimensional progressive collapse analysis of reinforced concrete frame structures subjected to sequential column removal", *Eng. Struct.*, **132**, 87-97.

Bjorhovde, R., Colson, A. and Brozzetti, J. (1990), "Classification system for beam-to-column connections", *J. Struct. Eng.*, **116**(11), 3059-3076.

Chan, S.L. and Chui, P.T. (2000), "Nonlinear static and cyclic analysis of steel frames with semi-rigid connections", Elsevier, Amsterdam, Netherlands.

Chen, C.H., Zhu, Y.F., Yao, Y., Huang, Y. and Long, X. (2016a), "An evaluation method to predict progressive collapse resistance of steel frame structures", *J. Constr. Steel Res.*, **22**, 238-250.

Chen, C.H., Zhu, Y.F., Yao, Y. and Huang, Y. (2016b), "Progressive collapse analysis of steel frame structure based on the energy principle", *Steel Compos. Struct.*, *Int. J.*, **21**(3), 553-571.

Chen, C.H., Zhu, Y.F., Yao, Y. and Huang, Y. (2016c), "The finite element model research of the pre-twisted thin-walled beam", *Struct. Eng. Mech.*, *Int. J.*, **57**(3), 389-402.

Chen, C., Zhang, Q., Keer, L.M., Yao, Y. and Huang, Y. (2018a), "The multi-factor effect of tensile strength of concrete in numerical simulation based on the Monte Carlo random aggregate distribution", *Constr. Build. Mater.*, **165**, 585-595.

Degertekin, S.O. and Hayalioglu, M.S. (2004), "Design of non-linear semi-rigid steel frames with semi-rigid column bases", *Electron. J. Struct. Eng.*, **4**, 1-16.

Federal Emergency Management Agency 356 (2000), Prestandard and Commentary for the Seismic Rehabilitation of Buildings; Washington D.C., USA.

Frye, M.J. and Morris, G.A. (1975), "Analysis of flexibly connected steel frames", *Can. J. Civil Eng.*, **2**(3), 280-291.

Fu, Q.N., Tan, K.H., Zhou, X.H. and Yang, B. (2017), "Numerical simulations on three-dimensional composite structural systems against progressive collapse", *J. Const. Steel Res.*, **135**, 125-136.

Ihaddoudene, A.N.T., Saidani, M. and Chemrouk, M. (2009), "Mechanical model for the analysis of steel frames with semi-rigid joints", *J. Constr. Steel Res.*, **65**(3), 631-640.

Jones, S.W., Kirby, P.A. and Nethercort, D.A. (1983), "The analysis of frames with semi-rigid connections—a state-of-the-art report", *J. Constr. Steel Res.*, **3**(2), 2-13.

Khuyen, H.T. and Iwasaki, E. (2016), "An approximate method of dynamic amplification factor for alternate load path in redundancy and progressive collapse linear static analysis for steel truss bridges", *Case Stud. Struct. Eng.*, **6**, 53-62.

Li, Y., Lu, X.Z., Guan, H. and Ye, L.P. (2014), "An energy-based assessment on dynamic amplification factor for linear static analysis in progressive collapse design of ductile RC frame structures", *Adv. Struct. Eng.*, **17**(8), 1217-1225.

Liu, M. (2013a), "A new dynamic increase factor for nonlinear static alternate path analysis of building frames against progressive collapse", *Eng. Struct.*, **48**, 666-673.

Liu, M. (2013b), "Discussion of "Alternate Path Method in Progressive Collapse Analysis: Variation of Dynamic and Nonlinear Load Increase Factors" by Aldo McKay, Kirk Marchand, and Manuel Diaz", *Pract. Period. Struct. Des. Constr.*, **21**(2), 07016001.

Liu, M. (2016), "Discussion of "Alternate Path Method in Progressive Collapse Analysis: Variation of Dynamic and Nonlinear Load Increase Factors" by Aldo McKay, Kirk Marchand, and Manuel Diaz", *Pract. Period. Struct. Des. Constr.*, **21**(2), 07016001.

Marjanishvili, S. and Agnew, E. (2006), "Comparison of various procedures for progressive collapse analysis", *J. Perform. Constr. Fac.*, **20**(4), 365-374.

Mashhadiali, N., Kheyroddin, A. and Zahiri-Hashemi, R. (2016), "Dynamic Increase Factor for Investigation of Progressive Collapse Potential in Tall Tube-Type Buildings", *J. Perform. Constr. Fac.*, **30**(6), 4016050.

Mirtaheri, M. and Zoghi, M.A. (2016), "Design guides to resist progressive collapse for steel structures", *Steel Comp. Struct.*, *Int. J.*, **20**(2), 357-378.

Qin, X., Wang, W., Chen, Y. and Bao, Y. (2016), "A special reinforcing technique to improve resistance of beam-to-tubular column connections for progressive collapse prevention", *Eng. Struct.*, **117**, 26-39.

Saberi, V., Gerami, M. and Kheyroddin, A. (2014), "Comparison of bolted end plate and T-stub connection sensitivity to component thickness", *J. Constr. Steel. Res.*, **98**, 134-145.

Tavakoli, H.R. and Kiakojouri, F. (2013), "Numerical study of progressive collapse in framed structures: A new approach for dynamic column removal", *Int. J. Eng. Trans A*: *Basics*, **26**(7), 685-692.

Tsai, M.H. (2010), "An analytical methodology for the dynamic amplification factor in progressive collapse evaluation of building structures", *Mech. Res. Commun.*, **37**(1), 61-66.

Tsai, M.H. (2012), "Assessment of analytical load and dynamic increase factors for progressive collapse analysis of building frames", *Adv. Struct. Eng.*, **15**(1), 41-54.

Unified Facilities Criteria (2009), Design of Buildings to Resist Progressive Collapse; (UFC4-023-03), Department of Defense, USA.

US General Services Administration (2013), Progressive Collapse Analysis and Design Guidelines for New Federal Office Buildings and Major Modernization Projects; GSA.

Wang, W., Fang, C., Qin, X. and Li, L. (2016), "Performance of practical beam-to-SHS column connections against progressive collapse", *Eng. Struct.*, **106**, 332-347.

Yang, B. and Tan, K.H. (2012), "Numerical analyses of steel beam–column joints subjected to catenary action", *J. Constr. Steel Res.*, **70**, 1-11.

Yang, B. and Tan, K.H. (2013), "Experimental tests of different types of bolted steel beam–column joints under a central-column-removal scenario", *Eng. Struct.*, **54,** 112-130.

CC